

Research Article Physics

Discharge structure of Ar/SF₆ inductively coupled plasma at high pressure

Shu-Xia Zhao*

Key Laboratory of Material Modification by Laser, Ion, and Electron Beams (Ministry of Education), School of Physics, Dalian University of Technology, 116024, Dalian, China

Abstract:

In the article, the discharge structure of Ar/SF₆ inductively coupled plasma at high pressure is studied. At high electronegativity, the island potential is formed at discharge initial stage, and most of plasma dynamics are occurred in the potential. The self-coagulation and diffusion of both ambi-polar type exist in the plasma. The plasma is torn by the competition of them and a blue sheath is appeared in plasma. The plasma potential collapses and the electron also self-coagulates. The electron then deviates from the Boltzmann equilibrium at the self-coagulation. The steady state discharge profile is a combined structure of island and flat-top model. The discharge separation by double layer is not important anymore at high pressure.

Keywords: Discharge Structure, Electronegative Plasma, Fluid Simulation, Self-Coagulation, Blue Sheath

INTRODUCTION

The discharge structure is important for people to understand the plasma source. In the electropositive plasma source, the parabola and Bessel spatial characteristics are calculated by analytic theory, which builds a reference for the fluid simulation of inertial gas discharge profile (Lieberman, 2025). In the electronegative plasma source, the discharge structure is predicted by analytic theory as well that is deduced by Lichtenberg et al (Lichtenberg, 1997). Basically, the parabola, ellipse and flat-top profiles of ion density are calculated, constructing the reference that is used to examine the experimental observation. Many early measured ion density profiles of electronegative plasma were hence compared to the models3-5 (Berezhnoj, 2000; Vender, 1995; Kaga, 2001). In the theory of electronegative plasma, the recombination is assumed never larger than the ionization in ion chemical dynamics. However, the

Correspondence:

Shu-Xia Zhao, Key Laboratory of Material Modification by Laser, Ion, and Electron Beams (Ministry of Education), School of Physics, Dalian University of Technology, 116024, Dalian, China, ORCID ID: 0000-0001-9270-7465;

Received Dates: August 08, 2025; Accepted Date: September 10, 2025; Published Date: September 15, 2025;

Published Date: September 15, 2025;

Cite this article as: Zhao SX, Discharge structure of Ar/SF inductively coupled plasma at high pressure, Glob. Open Access J. Sci, 2025; 1(1):34-45.



negative chemical source is often seen in our recent fluid simulation of electronegative plasma (Zhao, 2021; Zhao & Li, 2021). Based on the negative source, we develop a self-coagulation theory (Tian, 2024). At the help of the new theory and the previous three models given at the assumption of positive source, we can successfully explain the discharge structure revealed by fluid simulation of different electronegative plasmas. In the References (Zhao, 2021; Zhao & Li, 2021), the comet structure of anion in the Ar/O2 inductively coupled plasma is revealed and explained. In the present article, we plan to interpret the structure of Ar/SF, inductively coupled plasma at high pressure, i.e., 90mTorr. In the future, the discharge structure of Ar/SF inductively coupled plasma at low pressure, 10mTorr, will be reported, where the discharge stratification, parabola profile and dielectric type double layer are described. The transport coefficients and electronegativities at low and high pressures are different, and the two discharge structures differ significantly.

METHODOLOGY

The fluid model includes the equations of electron, heavy species, electromagnetic field and the Poisson's equation. The equations are coupled together and solved by finite element numeric method. The inductively coupled plasma reactor consists of matching box, dielectric window and discharge chamber. It is powered by the 13.56MHz power source and worked in a pure H discharge mode. The chemical reaction of Ar/ SF_6 plasma includes the electron-impact reactions and heavy species reactions. The large SF_6 molecule is deeply fragmented and many neutrals, cations and anions are thus created. Besides for the fluid model, the theory of self-coagulation is built at analytically solving the quasi-Helmholtz equation. More detail of methodology can be found in the Reference (Tian, 2024).

RESULTS AND DISCUSSION

Formation of Island Potential Barrel

High pressure provides large electronegativity, and the electron is substantially depleted by attachment loss. As shown in Figure 1, at the discharge initial, the initially-set uniform electron density profile is swiftly shrunk to the coil, where the electron heating rate is high. Figure 2 shows the net source of electron in the stage. It is seen that at the beginning, the negative source is dominant until all the numerically designed electrons are consumed (this design does not influence the simulation reliability). Meanwhile, one island type of positive electron source is appeared under the coil, due to the intense ionization happened (the energy deposition into plasma from the power source is being conducted therein). This island type of source is ordinarily seen in gaseous discharge fluid simulation, and in electropositive plasma of the pressure range (e.g., 100mTorr), it leads to the wide profile of ambi-polar diffusion potential (Zhao, 2009). Nevertheless, herein, the electrons generated from the positive source cannot diffuse far away from the source at strong attachment loss. Correspondingly, the island potential is given at the limited diffusion (in Figure 3), different with the electropositive plasma. Though the shape is different, the island potential formed in the stage is ambi-polar diffusion potential since the electron is satisfied with the Boltzmann relation, given in Figure 4.

Self-coagulation of the Anion

In Figure 5, the total anions density at a certain position versus the simulating time is given. The radial and axial coordinates of the position are (8.4, 12.04), in a unit of centimeter. The position is hence selected because we prefer to observe the density temporal trend within the island potential barrel. It is seen that the anion density increases suddenly and swiftly in a time range of nearly from 10^{-5} s to 10^{-4} s, implying the occurrence of certain mechanism in the Ar/SF, plasm, i.e., self-coagulation of the anion. The mechanism is early reported in the References (Zhao, 2021; Zhao & Li, 2021; Tian, 2024), and found existing generally in the electronegative inductively coupled plasmas. As these early works exhibited, the formation of selfcoagulation needs two conditions, free diffusion and negative chemical source. The fluid simulation above shows that at high pressure, the island potential is formed at the coil, where the electron-impact reactions are intensively occurred, e.g., ionization, attachment and ionic recombination. It implies that the potential and reaction centers coincide. So, at the center, plasma species are freely diffused. The negative source led to by the ionic combination is given in the Figure 6,

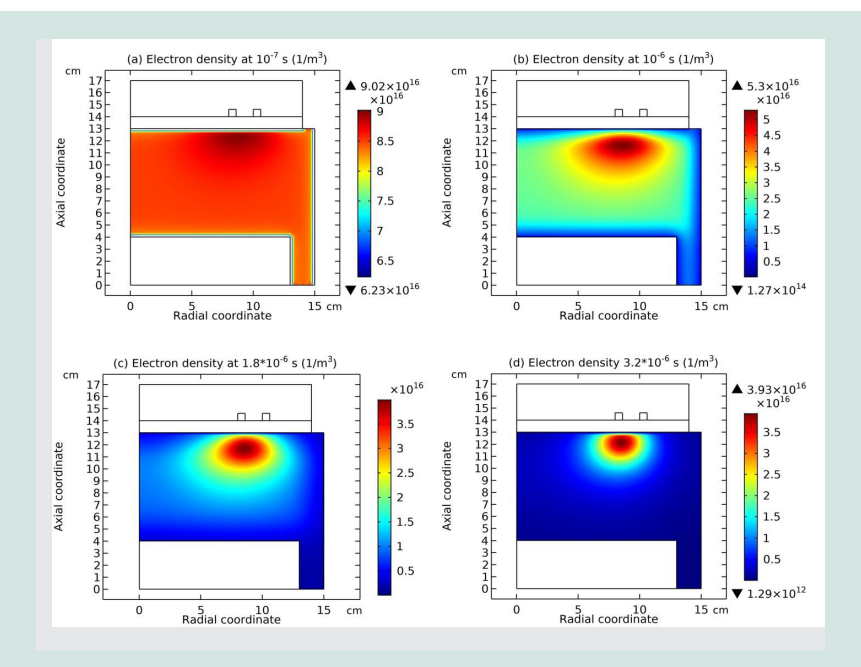


Figure 1: Electron densities of Ar/SF $_6$ inductively coupled plasma in an early stage of discharge, plotted at (a) 10^{-7} s , (b) 10^{-6} s , (c) 1.8×10^{-6} s , and (d) 3.2×10^{-6} s , respectively. The data are given by the fluid simulation, at the discharge condition of 300W, 90mTorr and 10% SF $_6$ content.

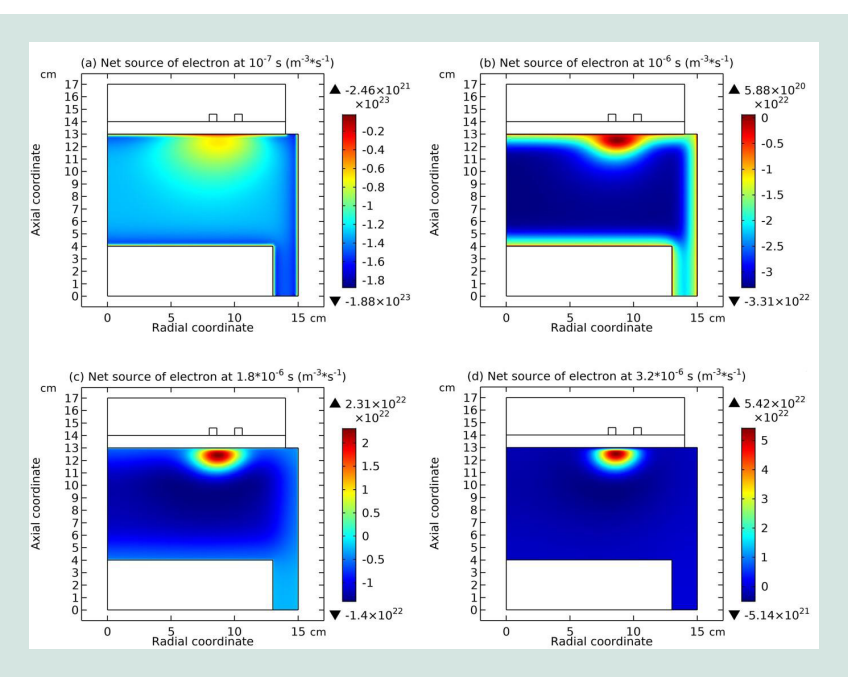


Figure 2: Electron net sources of Ar/SF $_6$ inductively coupled plasma in an early stage of discharge, plotted at (a) 10^{-7} s , (b) 10^{-6} s , (c) 1.8×10^{-6} s , and (d) 3.2×10^{-6} s , respectively. The data are given by the fluid simulation, at the discharge condition of 300W, 90mTorr and 10% SF $_6$ content.

where the summed anions density and the net source of them before and after the self-coagulation process are both compared. Due to the shielding of island potential, anions generated cannot escape, but directly recombine with the cation, and along with the density increase, the recombination rate increases as well, even faster, eventually leading to the negative source. The self-coagulation can increase up the anion density, as

reported in the References (Zhao, 2021; Zhao & Li, 2021; Tian, 2024). See Figure 6(a,b) for better reference.

It is seen that the self-coagulation precursor is chemical reaction, and so it behaves more like a chemistry process, different to the ambi-polar diffusion or double layer that is essentially a result of electric interaction. Therefore, although the basic shape of anion density before and after the self-coagulation is an

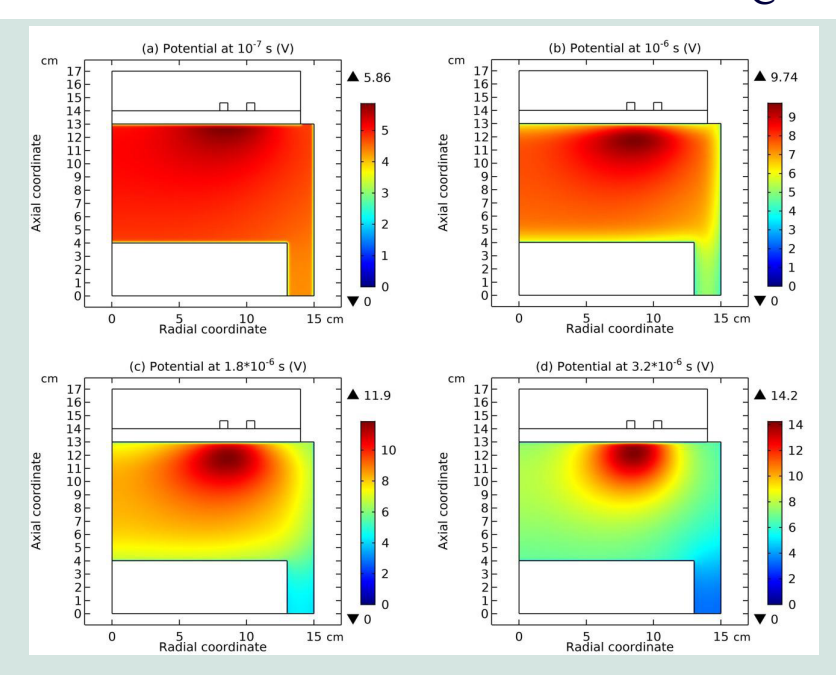


Figure 3: Plasma potentials of Ar/SF $_6$ inductively coupled plasma in an early stage of discharge, plotted at (a) 10^{-7} s , (b) 10^{-6} s , (c) 1.8×10^{-6} s , and (d) 3.2×10^{-6} s , respectively. The data are given by the fluid simulation, at the discharge condition of 300W, 90mTorr and 10% SF $_6$ content.

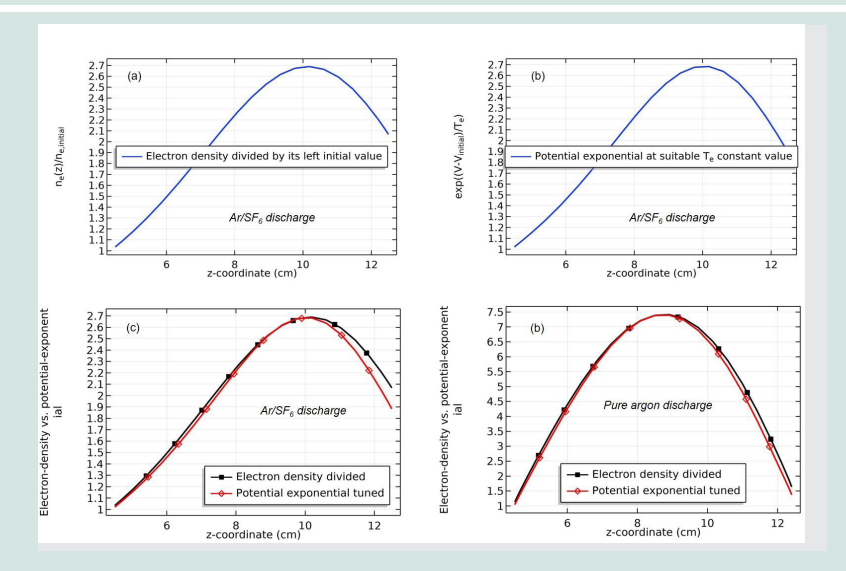


Figure 4: Plasma potentials of Ar/SF $_6$ inductively coupled plasma in an early stage of discharge, plotted at (a) 10^{-7} s , (b) 10^{-6} s , (c) 1.8×10^{-6} s , and (d) 3.2×10^{-6} s , respectively. The data are given by the fluid simulation, at the discharge condition of 300W, 90mTorr and 10% SF $_6$ content.

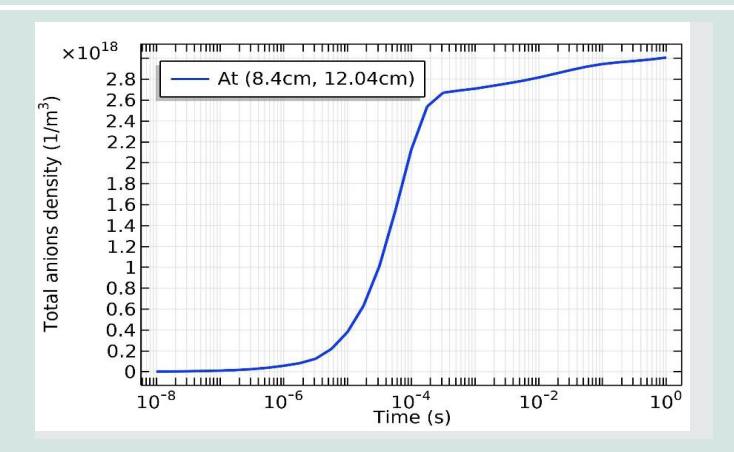


Figure 5: Plasma potentials of Ar/SF $_6$ inductively coupled plasma in an early stage of discharge, plotted at (a) 10^{-7} s , (b) 10^{-6} s , (c) 1.8×10^{-6} s , and (d) 3.2×10^{-6} s , respectively. The data are given by the fluid simulation, at the discharge condition of 300W, 90mTorr and 10% SF $_6$ content.

island, their tiny border behaviors, especially under the dielectric window, are different. As being enlarged in Figure 7, the border before the process is steep and it is softened after the process. The steep border, we believe, is given by the squeezing of adjacent double layer that is an external force, but the soft border is led to by the centric coagulation, i.e., one internal force. At compared to the self-coagulation, the island potential is more like the external force as well since its electric field force is strong at the peripheral region of barrel.

Ambi-polar Self-coagulation and Blue Sheath

In the high electronegative plasma such as the Ar/SF plasma considered, to satisfy the electric neutrality, the cation needs to coagulate as well. Then how does the cation self-coagulate? When checking the transport equation of self-coagulation shown in the Eq. (3.1) that consists of free diffusion and negative source, we see that the polarity is not important anymore. At the potential center, the cation free diffusion is dominant, and the recombination leading negative source is applicable to both the anion and cation. So, at the bottom, the cation is also self-coagulated. Although the polarity is of no significance in the self-coagulation itself, the origin of self-coagulation, i.e., recombination, is indeed given by the cation and anion that hold positive and negative polarity, respectively. So, the self-coagulations of anion and cation can be defined as an ambi-polar type, similar to the definition of ambi-polar diffusion. As reported in the Reference (Zhao & Li, 2021) and herein the appendix, the recombination source can play the role of virtual potential that drift species, so the dynamic balance between the diffusion and virtual drift is obtained and the simulation can reach to a steady state, i.e., plasma is not collapsed by endless recombination but stable density bumps of cation and anion are given (like a mass point). Furthermore, the recombination does not consume the cation and anion significantly since the electron still plays the predominant role and electronimpact reactions are continued to happen, which supplies source species persistently. In a word, the self-coagulation is complex process that couples many physics fields and can only be understand when taking into account the roles of all fields.

$$\frac{\partial n_{-}}{\partial t} - D_{-} \nabla^{2} n_{-} = -n_{-} v_{rec}.$$
..(3.1)

Up to now in the simulation, the cation and electron cooperatively build the island ambi-polar diffusion potential that disperses plasma components, cation and electron. Meanwhile, the anion and cation are selfcoagulated within the island bottom, which represents the accumulation process of plasma component. The dispersion process tends to create the continuous plasma medium, while the accumulation tends to create the plasma mass point that is discrete. These are two opposite physics. Not as in the electropositive plasma, the cation herein is in charge of two processes, selfcoagulation and diffusion of ambi-polar type. If the electronegativity is not high, the self-coagulation and diffusion of ambi-polar type can be balanced, and a new type of Boltzmann equilibrium of cation is achieved. At the balance location, the cation transport stops and the flux is zero, as reported in a relatively low electronegative plasma, Ar/Cl2 plasma (Zhao, 2025). But, here in the Ar/SF₆ plasma where the electronegativity is rather high, the self-coagulation dominates over diffusion. The predominant self-coagulation grabs and transmits the cation to the density bump area and hence leaves a local negatively charged region. Hence, the electrically neutral plasma is torn by the self-coagulation and electronegative sheath is appeared around the self-coagulated density bump in Figure 8. The electronegative sheath is also called blue sheath since the color is blue when it is observed in the charge density color map. This is less related to the anion since it has at the beginning been constricted in the potential bottom. The tearing movement of plasma has a significant influence on the ambi-polar island potential since fraction of cations are forced to betray (see further). At the same time, the self-coagulation and diffusion of ambi-polar type are separated by the blue sheath in Figure 8.

Collapse of Island Potential and Self-coagulation of Electron

In the highly electronegative Ar/SF₆ plasma considered here, the important fraction of cations that are in the potential center are forced to exclusively participate

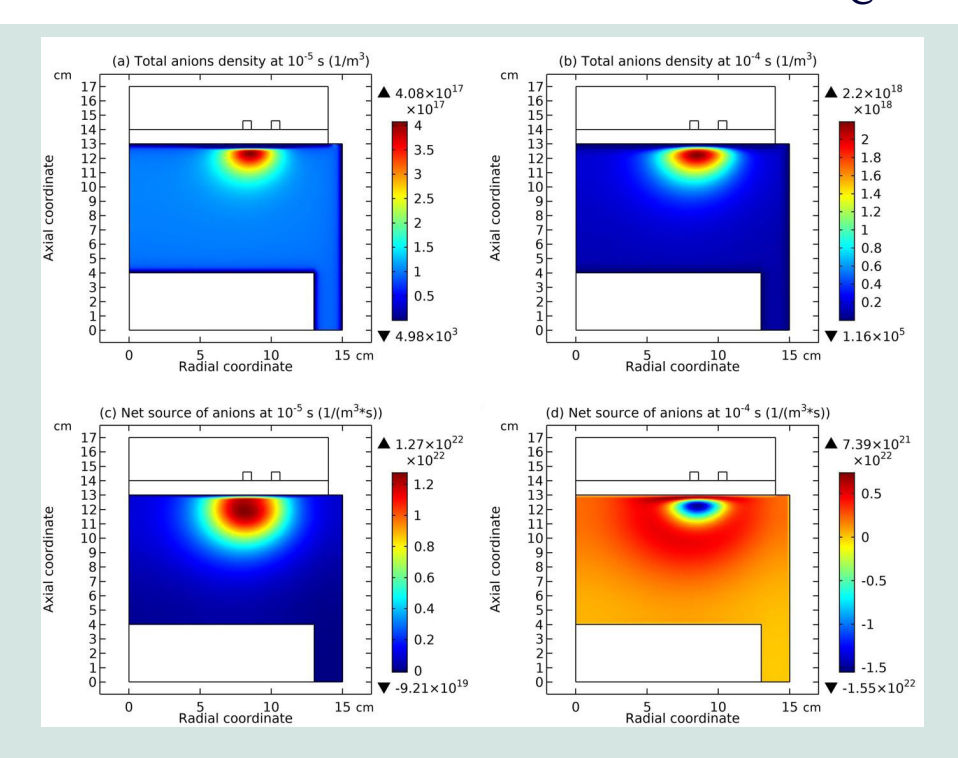


Figure 6: Total anions density at (a) 10^{-5} s and (b) 10^{-4} s, i.e., before and after the self-coagulation process, and net source of anions (c,d) at the two times. The data are given by the fluid simulation of Ar/SF₆ inductively coupled plasma, at the discharge condition of 300W, 90mTorr and 10% SF₆ content.

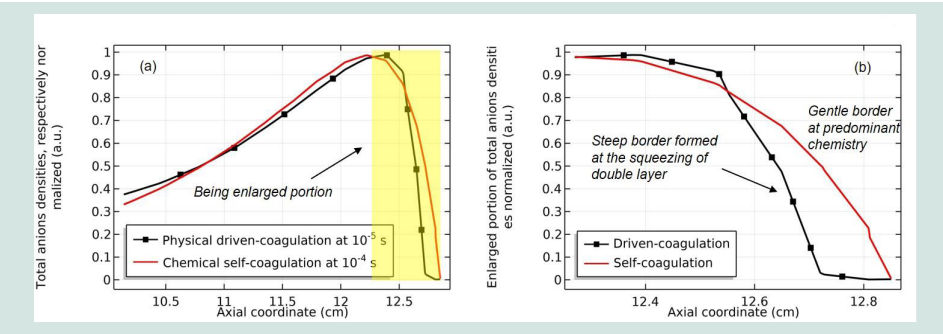


Figure 7: (a) Partial axial profiles of total anions densities normalized at their own maximum at two times, 10⁻⁵ s and 10⁻⁴ s. In (b), the enlarged portion of anions density profiles close to the dielectric window is shown. The data are given by the fluid simulation of Ar/SF₆ inductively coupled plasma, at the discharge condition of 300W, 90mTorr and 10% SF₆ content.

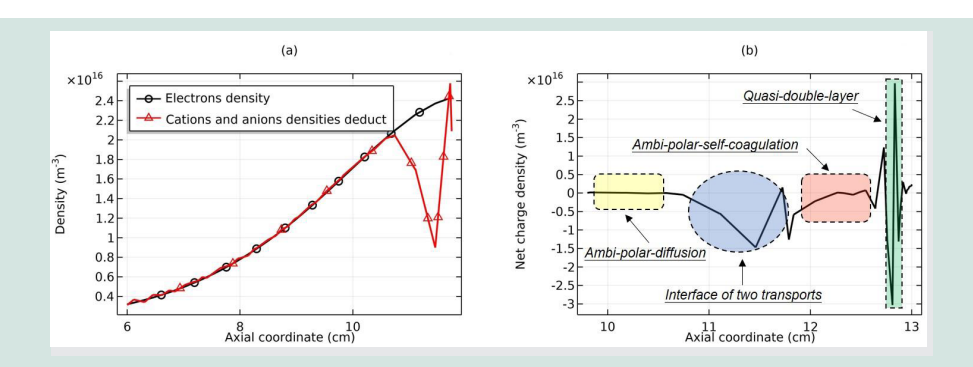


Figure 8: (a) Axial profiles of electron density and deduct of cations and anions densities, and (b) net charge density axial profile. In (b), the ambi-polar diffusion, ambi-polar self-coagulation and the interface, i.e., the blue sheath, are clearly seen. The discharge condition is the same as in Figure 7.

in the self-coagulation process and hence the island potential is collapsed due to the betrayal of these cations in Figure 9. Figure 10 shows the axial profile of potential versus time. It is seen that the potential is not totally broken and the potential value is kept at the electron temperature magnitude. This is because the electron still plays the important role in the discharge and the cations at the potential periphery are left available for sustaining the residual ambipolar diffusion potential.

Along with the potential collapse, the electron density profile is expanded, as shown in Figure 11. This is logic since the electron is weakly constricted at loosen potential. Meanwhile, the electron density deviates from the Boltzmann relation in Figure 12. This deviation is very interesting, for it represents the self-coagulation of electron. The potential collapses and then the electron quasi-freely diffuses. Moreover, far away from the positive electron source under the coil, clear negative chemical source of electrons is seen from the Figure 13, as it is known a strong electronegative discharge case herein. These two conditions mentioned lead to the self-coagulation of electron. The self-coagulation is one self-organization behavior (Zhao, 2021; Kadomtsev, 1992; Hayashi, 1999; Almeida, 2011), unrelated to the polarity and mass of considered species. At the low pressure, e.g., 10mTorr, the electron of Ar/SF₆ plasma is perfectly satisfied with the Boltzmann balance in Figure 14. This is because the discharge condition of 10mTorr Ar/SF, plasma does not meet the requirement of self-coagulation of electron. At first, the potential is ambi-polar at the electropositive edge. Second, the negative source of electron is not achieved at low electronegativity, as shown in Figure 15. Figure 15 still lists the net sources of anion and electron of Ar/SF, plasma of different pressures from 10mTorr to 90mTorr. As seen, the negative sources of negatively charged plasma species are easily formed, indicating that self-coagulation happens once the free diffusion is given. In conclusion, the self-coagulation phenomenon is very popular in the electronegative discharge, waiting the recognition of people.

Steady State Discharge Profile

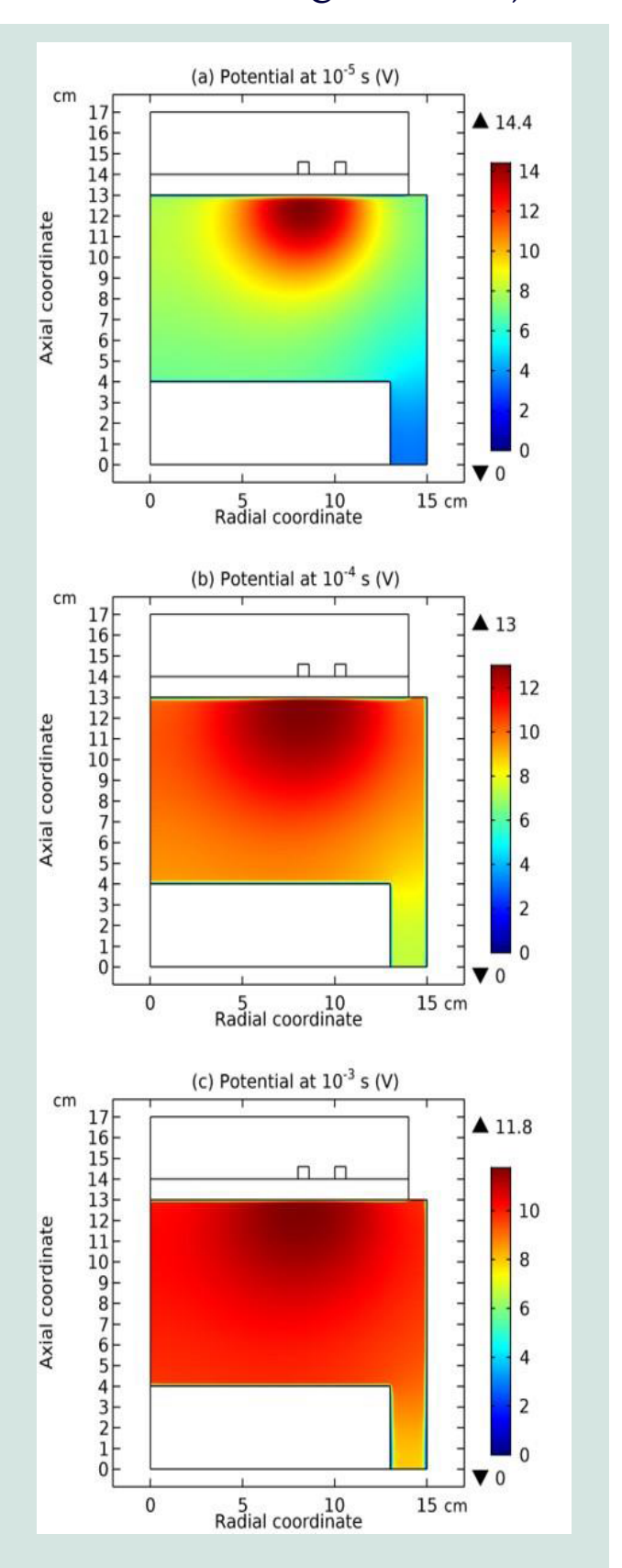


Figure 9: Plasma potential profile plotted at (a) $10^{-5} \, \mathrm{s}$, (b) $10^{-4} \, \mathrm{s}$, and (c) $10^{-3} \, \mathrm{s}$, respectively. Along with the ambi-polar self-coagulation, the centric potential value is decreased and the gradient is attenuated. The data are given by the fluid simulation of Ar/SF $_6$ inductively coupled plasma, at the discharge condition of 300W, 90mTorr and $10\% \, \mathrm{SF}_6$ content.

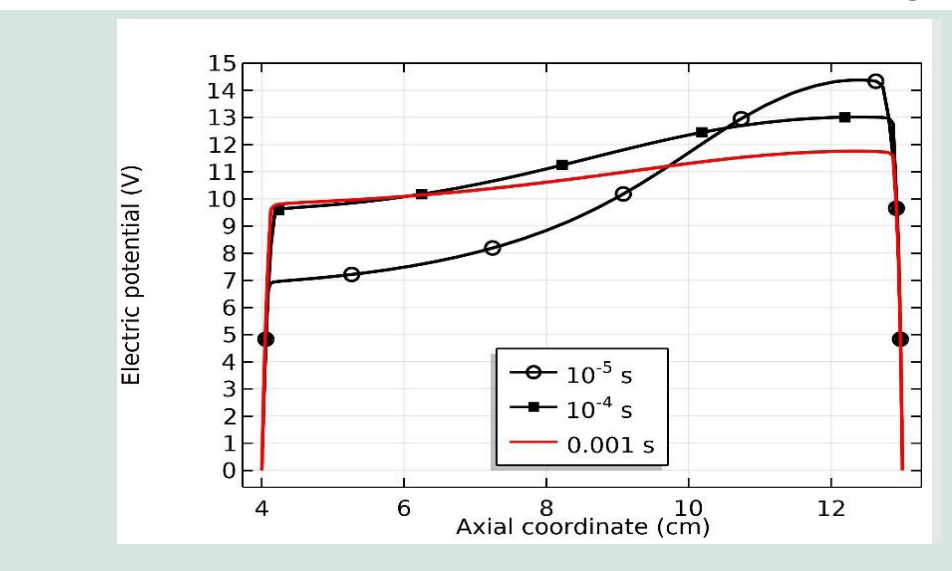


Figure 10: Axial potential profile at 10^{-5} s, 10^{-4} s, and 10^{-3} s, respectively, at the radial location of r=8cm. The data are given by the fluid simulation of Ar/SF₆ inductively coupled plasma, at the discharge condition of 300W, 90mTorr and 10% SF₆ content

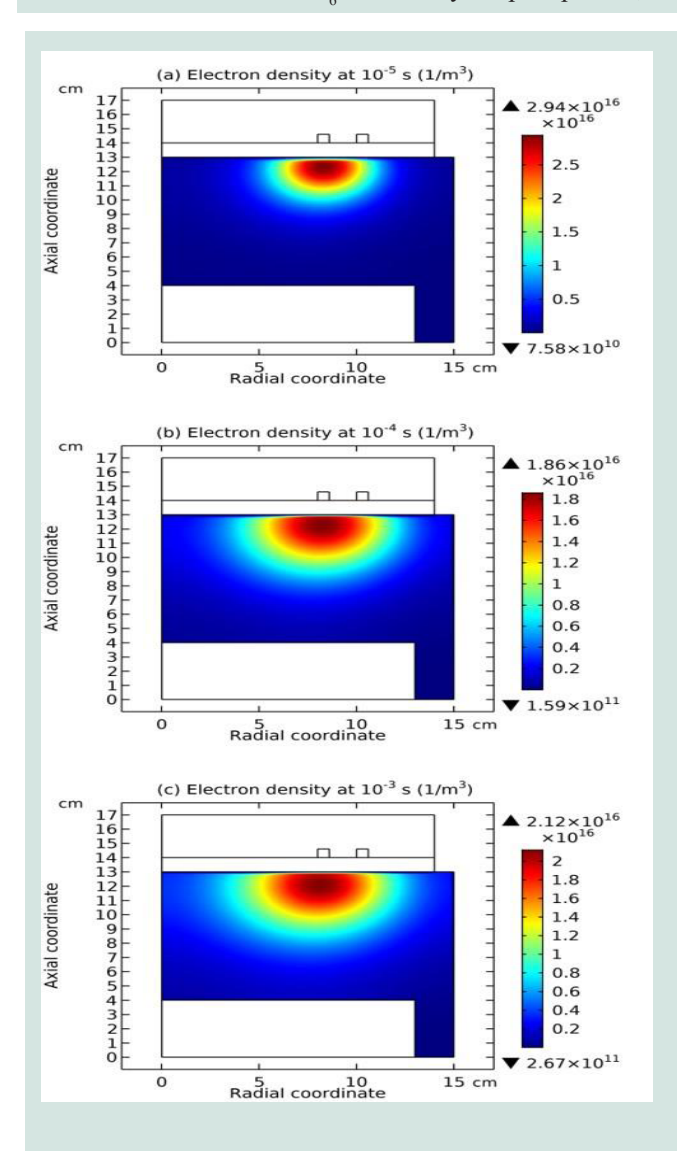


Figure 11: Electron densities at 10^{-5} s, 10^{-4} s, and 10^{-3} s, respectively. The electron density profile is expanded along with the self-coagulation of ambi-polar type. The data are given by the fluid simulation of Ar/SF₆ inductively coupled plasma, at the discharge condition of 300W, 90mTorr and 10% SF₆ content.

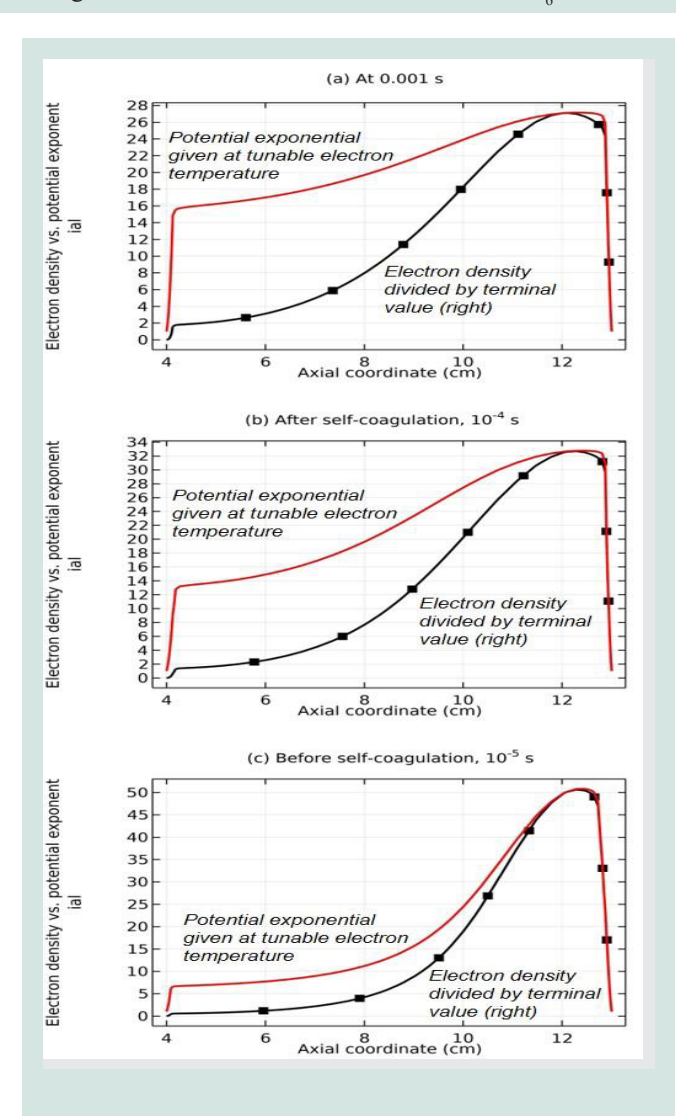


Figure 12: Electron density and Boltzmann balance check at different times, after self-coagulation of anion. The data are given by the fluid simulation of Ar/SF_6 inductively coupled plasma, at the discharge condition of 300W, 90mTorr and 10% SF_6 content.

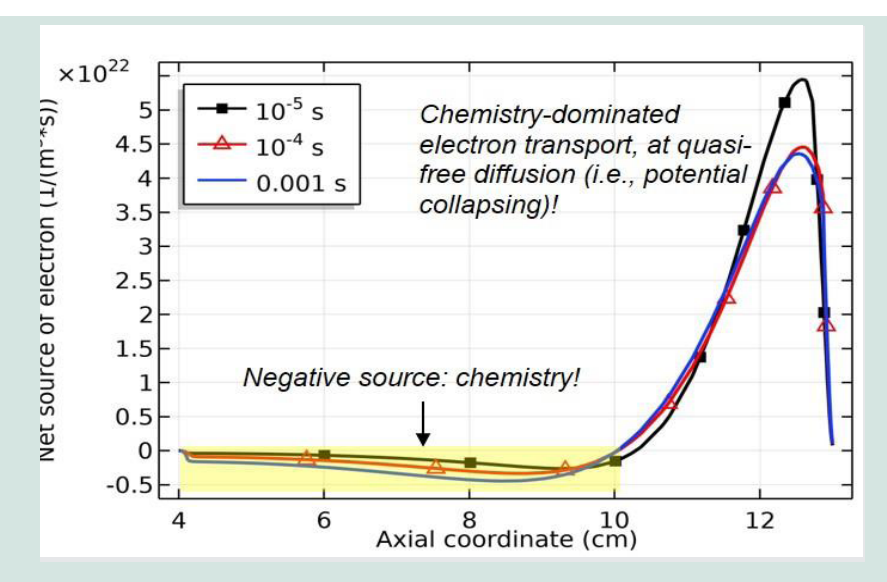


Figure 13: Axial profile of net source of electron at different times, after self-coagulation of anion. The data are given by the fluid simulation of Ar/SF₆ inductively coupled plasma, at the discharge condition of 300W, 90mTorr and 10% SF₆ content.

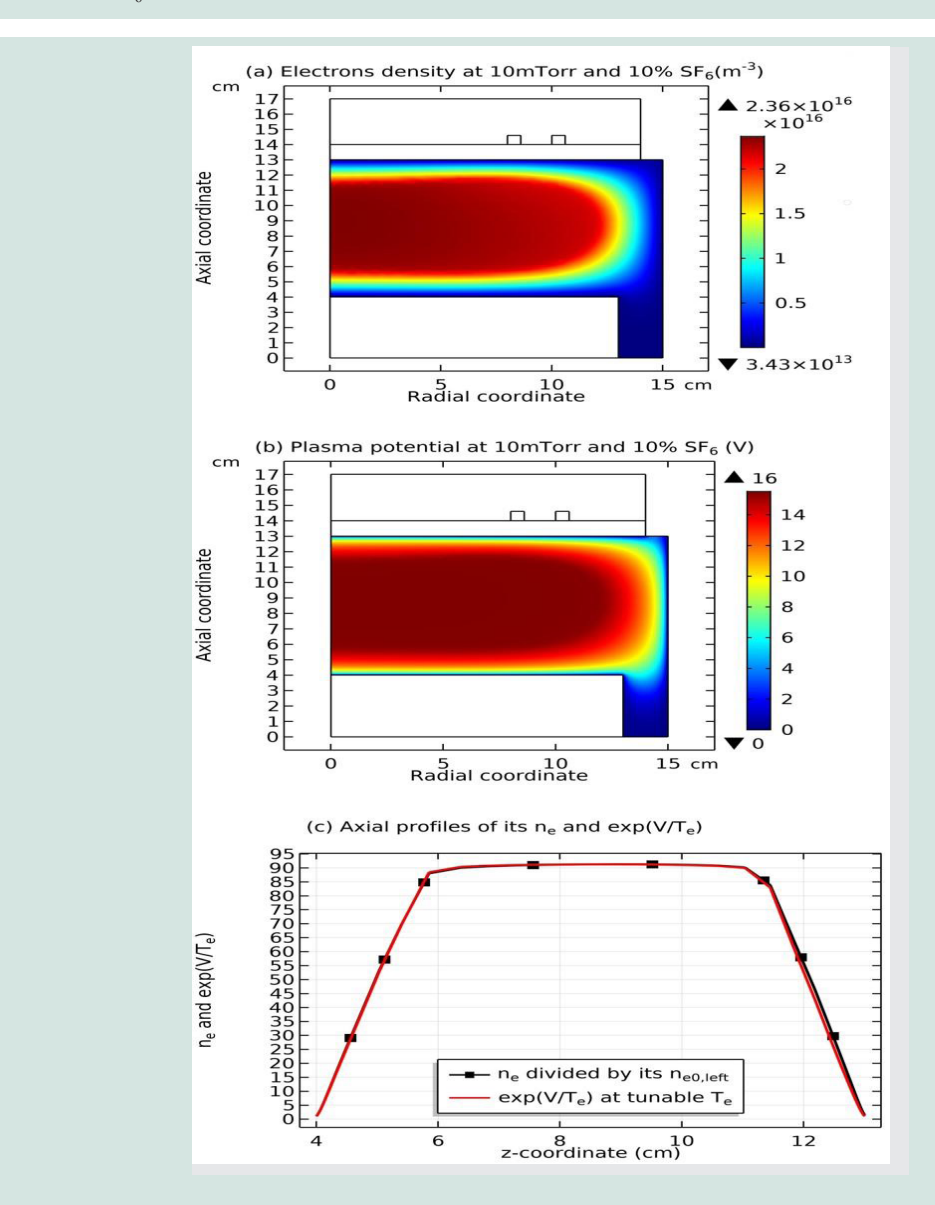


Figure 14: Electron density (a), plasma potential (b) and their Boltzmann relation inspection (c) at 10mTorr, at the other discharge condition of 300W and 10% SF₆ content, given by fluid model simulation. Electrons of Ar/SF₆ inductively coupled plasma obey the Boltzmann relation perfectly at low pressure.

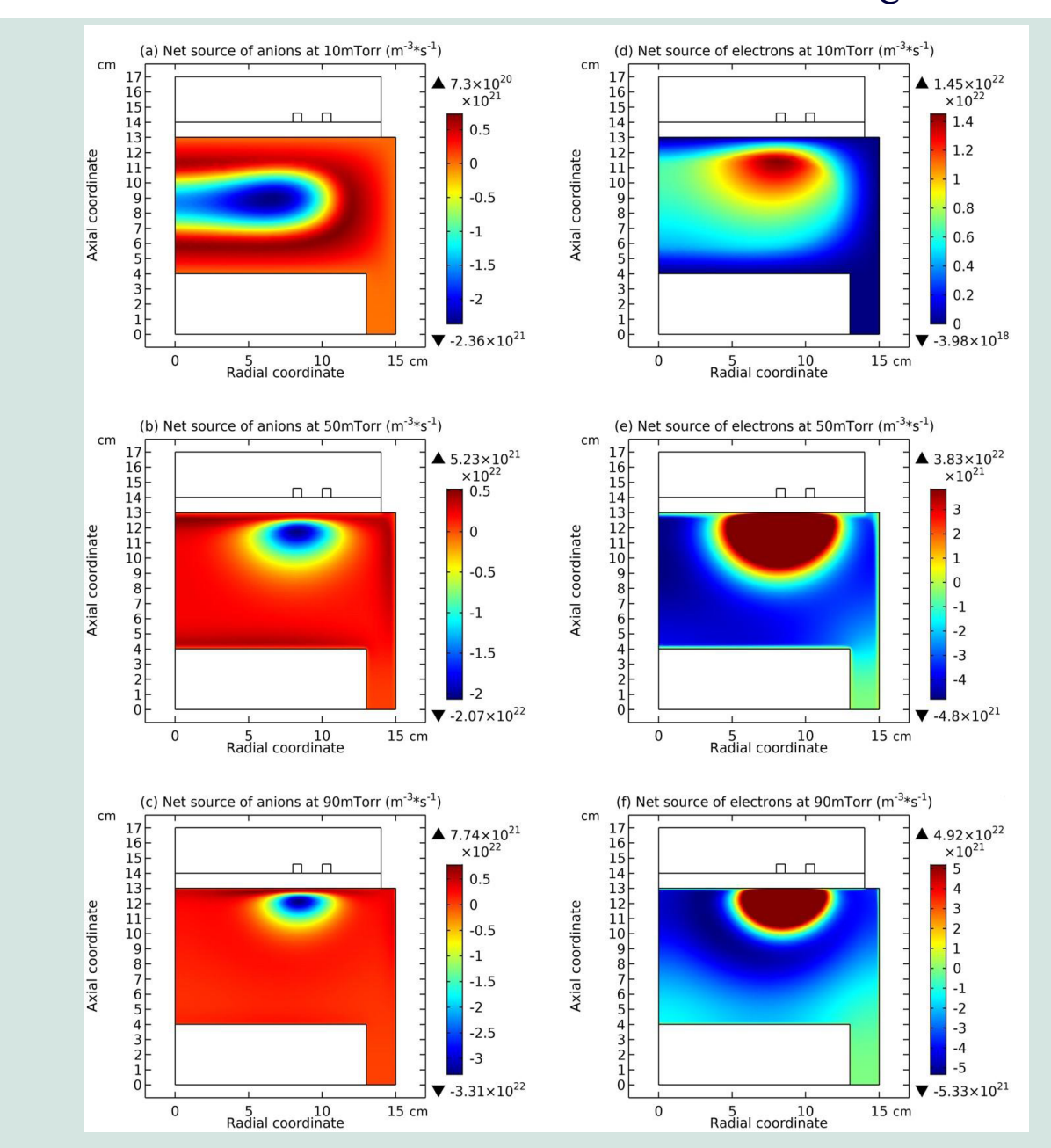


Figure 15: Pressure dependence of net sources of anions (a-c) and electron (d-f) of Ar/SF₆ inductive plasma, given by the fluid model simulation at the discharge condition of 300W and 10% SF₆ content.

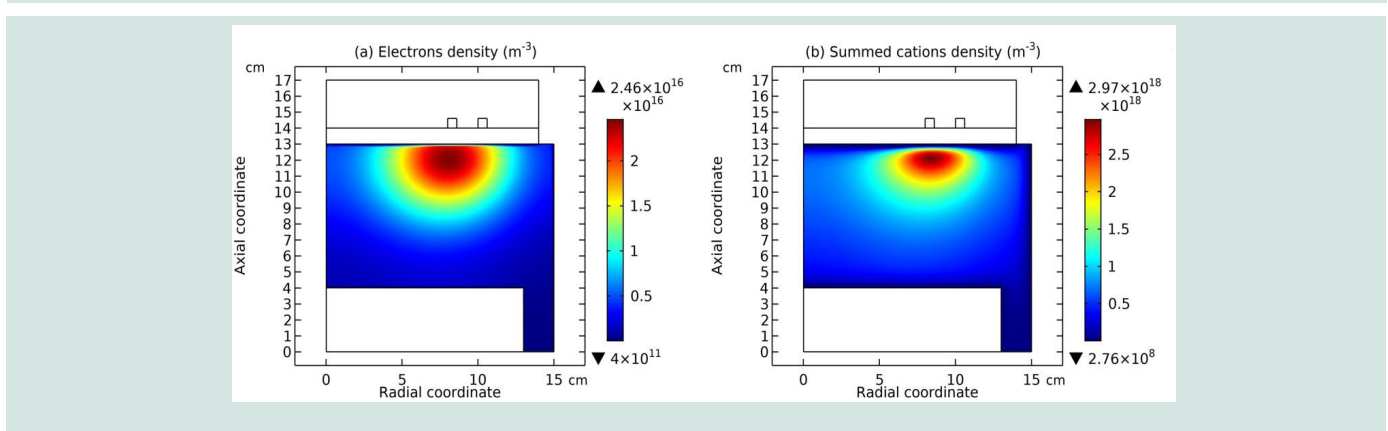


Figure 16: Steady state electron (a) and summed cations (b) densities of Ar/SF_6 inductively coupled plasma, at the discharge condition of 90mTorr, 300W and 10% SF_6 content, given by fluid model simulation.

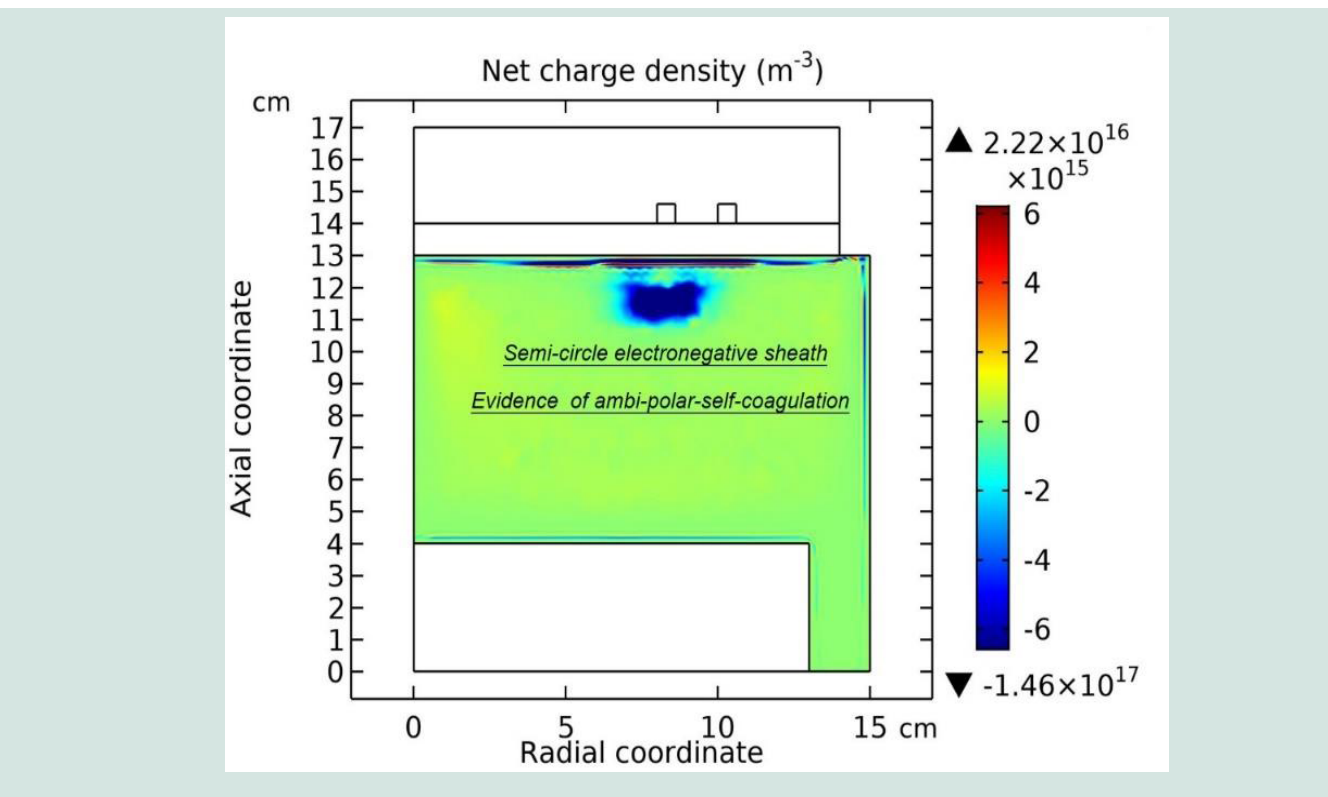


Figure 17: Net charge density of Ar/SF₆ inductively coupled plasma, at the discharge condition of 90mTorr, 300W and 10% SF₆ content, given by fluid model simulation.

The previous sections depict the temporal behavior of Ar/SF inductively coupled plasma at high pressure. In the process, many interesting mechanisms are revealed. In the section, the steady state discharge profile of the plasma is given. In Figure 16, the electron density and summed cations density are plotted. At the high electronegativity, the basic shape of the two profiles is island. At the potential collapse, the electron density profile is wider than the cation that undergoes the strong self-coagulation under the coil. The anion density profile is similar to the cation because of the ambi-polar self-coagulation. Except the island bump, the cation density background is flat, in accordance to the analytic work prediction of Lichtenberg et al, i.e., flat-top model (Lichtenberg, 1997). In Figure 17, the charge density of the plasma is plotted. The blue sheath is seen around the density bump of ions.

CONCLUSION

In the work, the discharge structure of Ar/SF_6 inductively coupled plasma is investigated by means of fluid simulation and self-coagulation theory, at high pressure. To fully understand the steady-state discharge structure given by self-consistent simulation, the detail

of plasma evolution with time is needed. At initial, the island potential is given by the strong attachment reaction that limits the ambi-polar diffusion process. In the island, the self-coagulation of anion is happened. At analyzing the self-coagulation theory, the ambi-polar type of self-coagulation is proposed. The diffusion and coagulation are opposite physics and compete with each other. The plasma is torn by their competition and blue sheath appears to separate the diffusion and coagulation. Since cation is forced to participate in the self-coagulation, the island potential is collapsed and the electron deviates from the Boltzmann relation at its own self-coagulation.

CONFLICT OF INTEREST

The authors have no conflicts to disclose.

DATA AVAILABLE STATEMENT

The data that support the findings of this study are available within the article.

REFERENCES:

• Almeida, P. G. C., Benilov, M. S., & Faria, M. J. (2011). Three-dimensional modeling of self-organization in DC glow microdischarges. IEEE transactions on Plasma Science, 39(11) 2190-2191.

https://doi.org/10.1109/TPS.2011.2148129

• Berezhnoj, S. V., Shin, C. B., Buddemeier, U., & Kaganovich, I. (2000). Charged species profiles in oxygen plasma. Applied Physics Letter, 77(6), 800-802.

https://doi.org/10.1063/1.1306637

- Hayashi T., & Sato, T. (1999). Self-organizing plasmas. Plasma Physics and Controlled Fusion, 41 A229-A238. https://doi.org/10.1088/0741-3335/41/3A/016
- Lichtenberg, A. J., Kouznetsov, I. G., Lee, Y. T., Lieberman, M. A., Kaganovich, I. D., & Tsendin, L. D. (1997). Modelling plasma discharges at high electronegativity. Plasma Sources Science and Technology, 6(3), 437-449. https://doi.org/10.1088/0963-0252/6/3/022
- Lieberman, M. A., & Lichtenberg A. J. (2005), Principles of plasma discharges and materials processing, New York: Wiley.

https://doi.org/10.1002/0471724254

• Kadomtsev, B. B. (1992). Self-organization and transport in Tokamak plasma. Plasma Physics and Controlled Fusion, 34(13) 1931-1938.

https://doi.org/10.1088/0741-3335/34/13/023

• Kaga, K., Kimura, T., Imaeda, T., & Ohe, K. (2001). Spatial structure of electronegative Ar/CF4 plasmas in capacitive RF discharges. Japanese Journal of Applied Physics, 40(10) 6115-6116.

https://doi.org/10.1143/JJAP.40.6115

• Tian, Y. & Zhao, S. X. (2024). Self-coagulation theory and related comet- and semi-circle-shaped structures in electronegative and gaseous discharging plasmas in the laboratory. Applied Science, 14, 8041.

https://doi.org/10.3390/app14178041

• Zhao, S. X. (2021). Quasi-delta negative ions density of Ar/O2 inductively coupled plasma at very low electronegativity. Chinese Physics B, 30(5) 055201.

https://doi.org/10.1088/1674-1056/abd16a

• Zhao, S. X., & Li, J. Z. (2021). Delta distribution of electronegative plasma predicted by reformed spring oscillator dynamic equation with dispersing force. Chinese Physics B, 30(5) 055202.

https://doi.org/10.1088/1674-1056/abd166

- Zhao, S. X., Tang, A. Q., & Tian, Y. (2005). Discharge structure of Ar/Cl2 inductively coupled plasma: A cyclic study of discharge conditions at fixed power. Journal of Technological and Space Plasmas, 1(1), 218-249. https://doi.org/10.31281/p8p08506
- Zhao, S. X., Xu, X., Li, X. C., & Wang, Y. N. (2009). Fluid simulation of the E-H mode transition in inductively coupled plasma. Journal of Applied Physics, 105(8) 083306.

https://doi.org/10.1063/1.3112009

• Vender, D., Stoffels, W. W., Stoffels, E., Kroesen, G. M. W., & Hoog, F. J. (1995). Charged-species profiles in electronegative radio-frequency plasma. Physical Review E, 51(3), 2436-2444.

https://doi.org/10.1103/PhysRevE.51.2436

©**2025** Zhao SX, et al. This is an open-access article distributed under the terms of the Creative Commons Attribution License 4.0 International License.

